Number-state filter for pulses of light

Nikolai Lauk[*] and Michael Fleischhauer
Department of Physics and Research Center OPTIMAS, University of Kaiserslautern, 67663 Kaiserslautern, Germany

We present a detailed theoretical analysis of a Fock-state filter based on the photon-number-dependent group delay in cavity-induced transparency proposed by Nikoghosyan and Fleischhauer [G. Nikoghosyan and M. Fleischhauer, Phys. Rev. Lett. **105**, 013601 (2010)]. We derive a general expression for the propagation velocity of different photon-number components of a light pulse interacting with an optically dense ensemble of three-level atoms coupled to a resonator mode under conditions of cavity-induced transparency. These predictions are compared to numerical simulations of the propagation of few-photon wave packets, and an estimation for experimental realization is made.

I. INTRODUCTION

Creation of nonclassical states of light is one of the central topics in quantum optics. Photon-number states, also called Fock states of light, are perhaps the most prominent representatives of those. They are of particular interest for quantum information processing as they can be used as a carrier of discrete bits of quantum information [1–3]. Despite the fact that by now there are many successful experimental realizations for the creation of single-photon states, e.g., in cavity-QED systems [4–10], an ideal single-photon source, i.e., a device that efficiently provides propagating single photons on demand, is still missing. An extremely useful tool would be a filter that allows one to extract different photon-number components of a propagating wave packet. Such a tool would provide several advantages over other systems. For example, it could also be used as a deterministic source for a many-photon state. A further advantage is the control of the pulse shape, since the single-photon shape will be inherited from the original coherent light pulse, which can be shaped more easily than a single-photon wave packet.

A proposal for such a system was made in [11], where a possibility of spatial separation of different photon-number components of an initially coherent pulse was shown. However, the theoretical analysis performed in [11] was based on nonlinear operator equations. To handle these, a couple of simplifying assumptions and approximations on the operator level had to be made. These are known to be difficult to justify in general. In this paper, we reexamine this system and provide a rigorous and quantitative analysis of the scheme, including an assessment of experimental requirements.

The proposed Fock-state filter is based on a phenomenon called cavity-induced transparency (CIT). It occurs in an ensemble of three-level atoms with a Λ-type configuration of couplings to two electromagnetic fields and is closely related to the well-known effect of electromagnetically induced transparency (EIT) [12]. The difference between the two systems is the replacement of the coherent control field in EIT by a quantized cavity mode. The coupling of the atomic ensemble to the cavity mode, even if it is in the vacuum state, can lead to transparency for the propagating probe field

in an otherwise opaque medium. Transparency induced by an empty cavity, called vacuum-induced transparency (VIT), was theoretically proposed in [13] and has been demonstrated experimentally in [14]. The interaction of the probe field with the coupled atom-cavity system leads to a temporary transfer of photons from the probe field to the cavity mode. The number of cavity photons is determined by the number of the probe field photons, and therefore is proportional to the probe field intensity. The backaction of the hybrid atom-cavity system onto the probe field, in particular its effect onto the group velocity, depends on the strength of the cavity field, i.e., on the number of cavity photons. As a consequence, different photon-number components of the probe field propagate with different velocities causing a photon-number-dependent group delay of the probe field. This process is analyzed in detail in this paper.

The paper is organized as follows. In Sec. II, we introduce the model, discuss the underlying principle of the system, and summarize the expected results based on intuition. Then, in Sec. III, we derive a general expression for the photon-number-dependent group velocity using the concept of dark states. To confirm these results, we have performed numerical wave-function simulations for up to two photons in the initial pulse, which we present in Sec. IV. Section V discusses consequences for experimental implementations and Sec. VI gives a summary and conclusions.

II. MODEL

We consider a gas consisting of three-level atoms in a Λ-type configuration [see Fig. 1(b)]. A cavity mode $\hat{a}_c$ couples the $|s\rangle - |e\rangle$ transition of the atoms, and the adjacent $|g\rangle - |e\rangle$ transition is coupled to a propagating quantum field described by the slowly varying operator

$$\hat{\mathcal{E}}(\mathbf{r},t) = \frac{1}{\sqrt{V}} \sum_{\mathbf{k}} \hat{b}_{\mathbf{k}} e^{i(\mathbf{k}\cdot\mathbf{r}-\omega_{\mathbf{k}}t)} e^{-i(k_p z - \omega_p t)}, \tag{1}$$

where $\hat{b}_{\mathbf{k}}$ is the annihilation operator of a photon in mode $\mathbf{k}$ with corresponding frequency $\omega_{\mathbf{k}}$, V is the quantization volume, and ω_p is the carrier frequency of the quantized probe field with corresponding wave number $k_p = \omega_p/c$ [see Fig. 1(a)]. Initially all atoms are assumed to be in the ground state $|g\rangle$ and the cavity mode is in the vacuum state. The Hamiltonian

_____
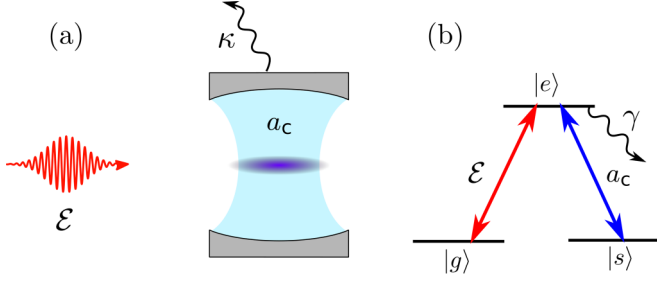[*]nlauk@physik.uni-kl.de

FIG. 1. (a) Setup of cavity-induced transparency with (b) corresponding atomic-level scheme. The probe field $\hat{\mathcal{E}}$ and cavity mode $\hat{a}_c$ couple to the transitions $|g\rangle - |e\rangle$ and $|s\rangle - |e\rangle$ from the atomic ground state $|g\rangle$ and metastable "spin" state $|s\rangle$ to a common excited state $|e\rangle$ in two-photon resonance.

of the system in a frame rotating with the probe field carrier frequency ω_p is given by

$$\hat{H} = \sum_{\mathbf{k}} \hbar(\omega_{\mathbf{k}} - \omega_p)\hat{b}_{\mathbf{k}}^\dagger \hat{b}_{\mathbf{k}} + \hbar \int d^3\mathbf{r}\, n(\mathbf{r})[\Delta\sigma_{ee}(\mathbf{r}) + \delta\sigma_{ss}(\mathbf{r})]$$

$$- \int d^3\mathbf{r}\, n(\mathbf{r})[g\sigma_{ge}(\mathbf{r})\hat{\mathcal{E}}^\dagger(\mathbf{r}) + G\sigma_{se}(\mathbf{r})\hat{a}_c^\dagger + \text{H.c.}], \quad (2)$$

where we introduced continuous atomic operators $\sigma_{lm}(\mathbf{r}) = \frac{1}{\Delta N}\sum_j^{\Delta N} |l_j\rangle\langle m_j|$ by averaging over small volume around $\mathbf{r}$ containing ΔN particles [15]. $n(\mathbf{r})$ is the atomic density, and Δ and δ denote the single-photon and two-photon detuning, respectively. $g = d_{ge}\sqrt{\frac{\omega_p}{2\hbar\epsilon_0}}$ and $G = d_{se}\sqrt{\frac{\omega_c}{2\hbar\epsilon_0 V_c}}$ are the single-atom coupling constants for the probe field and cavity field, respectively, where d_{ge} and d_{se} are dipole matrix elements of the $|g\rangle - |e\rangle$ and $|s\rangle - |e\rangle$ transitions, and V_c is the cavity quantization volume.

The first line in (2) describes the free evolution of the atomic system and the propagating probe field and the second line describes the interaction between them. Note that the free Hamiltonian of the cavity mode vanishes in the chosen rotating frame.

To get some intuition for the operation of the Fock-state filter, let us first consider the EIT case. There the atomic transition $|s\rangle - |e\rangle$ is coupled by the classical driving field with Rabi frequency Ω. This coupling induces transparency for the probe field on the otherwise opaque transition $|g\rangle - |e\rangle$. In addition, the group velocity of the probe field is modified [15] according to

$$\frac{v_g}{c} = \frac{\Omega^2}{g^2 n + \Omega^2}, \quad (3)$$

and depends on the strength of the control field Ω and on the collective atom-field coupling $g\sqrt{n}$. Now by replacing the driving field with a cavity, it seems natural that the group velocity will depend on the effective atom-cavity coupling $G\sqrt{N}$, where N is the number of photons in the cavity. Thus we expect that for strong backaction of the atom-cavity system onto the probe field, which happens in the strong-coupling regime, i.e., for a single-atom cooperativity $C = G^2/\gamma\kappa > 1$, different photon-number component will propagate with different group velocities. Here, κ and γ are the decay rates of the cavity and the atomic polarization, respectively.
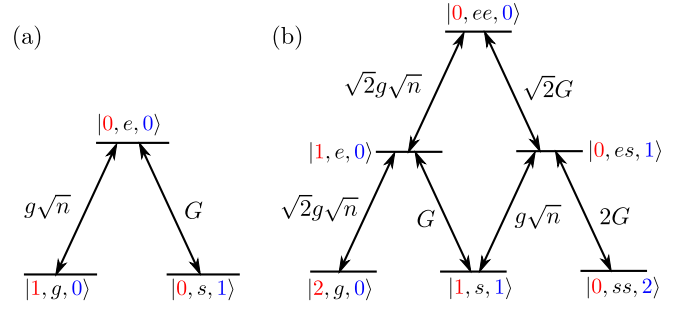

FIG. 2. Participating levels and corresponding coupling schemes for the (a) single- and (b) two-excitation manifolds.

III. GROUP VELOCITY

To become more acquainted with the system and to introduce the key concept of dark states, let us first consider a related toy model, where we consider the probe field as a single-mode cavity field $\hat{\mathcal{E}} = \hat{b}/\sqrt{V}$. For the sake of simplicity, we set all detunings to zero. The corresponding Hamiltonian is then given by

$$\hat{H} = -\hbar \sum_{i=1}^{N_a} \left(g\sigma_{ge}^i \frac{\hat{b}^\dagger}{\sqrt{V}} + G\sigma_{se}^i \hat{a}_c^\dagger + \text{H.c.} \right), \quad (4)$$

where the sum runs over all interacting atoms N_a.

It is easy to verify that this Hamiltonian conserves the total number of excitations, i.e., the Hilbert space splits into decoupled manifolds, each of which contains all states with fixed excitation number (Fig. 2), and we can treat each manifold separately. By looking on the spectrum of (4) in different manifolds, we note that all of these manifolds have in common the existence of an eigenstate with eigenvalue zero, i.e., the so-called dark state. It is convenient to introduce the following notation for the interacting states $|n_s, e^l s^m, n_c\rangle$, where n_s and n_c denote the number of the probe field photons and cavity photons, respectively, and $e^l s^m$ denotes the atomic state that interacts with the probe and cavity fields and contains l atoms in state $|e\rangle$, m atoms in state $|s\rangle$, and all the other atoms in the ground state $|g\rangle$. Using this notation, we can express the dark state in the single-excitation manifold as

$$\left|\psi_D^{(1)}\right\rangle = \frac{G}{\sqrt{G^2 + g^2 n}}|1_s, g, 0_c\rangle - \frac{g\sqrt{n}}{\sqrt{G^2 + g^2 n}}|0_s, s, 1_c\rangle. \quad (5)$$

Here, $g\sqrt{n}$ is the collective coupling strength of N_a atoms in a volume V with homogeneous density $n = N_a/V$ to the mode $\hat{b}$. The dark state for the subspace containing two excitations is given by

$$\left|\psi_D^{(2)}\right\rangle = \frac{1}{\mathcal{N}}(\sqrt{2}G^2 |2_s, g, 0_c\rangle - 2Gg\sqrt{n}\,|1_s, s, 1_c\rangle$$

$$+ g^2 n\,|0_s, ss, 2_c\rangle), \quad (6)$$

where $\mathcal{N} = \sqrt{2G^4 + 4G^2 g^2 n + g^4 n^2}$ is the normalization constant.

Note that in the low-excitation limit, i.e., if the number of excitations is much smaller than the number of atoms, atomic excitation can be treated as a bosonic excitation. As a consequence, the coupling of the state $|0_s, ss, 2_c\rangle$ to the upper

state $|0_s,es,1_c\rangle$ experiences a *twofold* bosonic enhancement, leading to a term $2G$ instead of $\sqrt{2}G$. Because of this *twofold* enhancement, we cannot write the double-excitation dark state as a direct product of two single-excitation dark states. This is different from the usual EIT, where the quantization of the control field is not considered and dark states can be represented as number states of a polariton operator [15].

The general expression for the dark state in the N-excitation subspace reads

$$|\psi_D^{(N)}\rangle = \frac{1}{\mathcal{N}} \sum_{M=0}^{N} f^M s^{N-M} |M_s,s^{N-M},(N-M)_c\rangle, \quad (7)$$

where $\mathcal{N}$ is the normalization constant and the coefficients are given by

$$f^M s^{N-M} = (-1)^M \frac{N!}{(N-M)!} \frac{1}{\sqrt{M!}} \left(\frac{G}{g\sqrt{n}}\right)^M. \quad (8)$$

Taking into account a possible decay from the excited atomic state $|e\rangle$, we find another feature of the dark states. Due to the fact that all of them do not contain contributions from the atoms in the excited state $|e\rangle$, the dark states are not affected by the decay from this state, which is the origin of their name. As a consequence, the dark states make up stationary states of the system in that case.

Let us proceed and consider the propagation of the probe field. To describe the propagation, we have to include many modes with different wave numbers $\mathbf{k}$, i.e., for a probe field propagating in the z direction, we can write $\hat{\mathcal{E}}(z) = \frac{1}{\sqrt{V}} \sum_k \hat{b}_k e^{ikz}$. Replacing the single-mode operator in (4) by this expression leads to a modification of the Hamiltonian according to

$$\hat{H} = -\hbar \sum_{i=1} g\sigma_{ge}^i \frac{1}{\sqrt{V}} \sum_k \hat{b}_k^\dagger e^{-ikz} + G\sigma_{se}^i \hat{a}_c^\dagger + \text{H.c.}$$
$$+ \sum_k \hbar\omega_k \hat{b}_k^\dagger \hat{b}_k, \quad (9)$$

where the additional part corresponds to the energy of the free probe field and gives rise to field propagation. We assume here an infinitely extended medium and ignore boundary effects. In this case, the system is translationally invariant and the Hamiltonian (9) does not couple modes with different k's.

We start again with a single-excitation case. Due to translational invariance, we can treat all k modes independently, i.e., for every mode k, we have three states $|1_k,g,0_c\rangle$, $|0_k,e_k,0_c\rangle$, and $|0_k,s_k,1_c\rangle$ coupled in a Λ configuration (compare Fig. 2), where we modified the previous notation by labeling it with the mode wave number k. Similar to the single-mode case, we can write, for the dark state of mode k,

$$|\psi_D^k\rangle = \frac{G}{\sqrt{G^2+g^2n}} |1_k,g,0_c\rangle - \frac{g\sqrt{n}}{\sqrt{G^2+g^2n}} |0_k,s_k,1_c\rangle. \quad (10)$$

States belonging to different k's are linearly independent and thus the dark state for the entire single-excitation manifold is given by

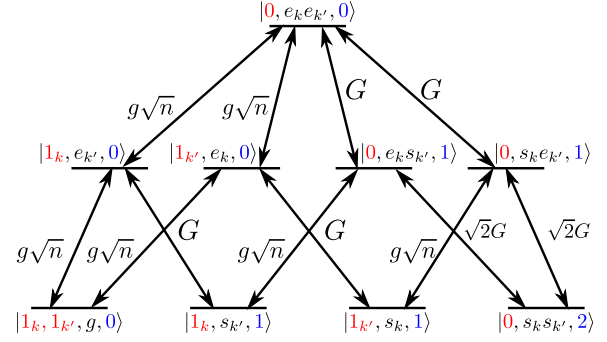$$|\psi_D\rangle = \sum_k C_k |\psi_D^k\rangle, \quad (11)$$

FIG. 3. Bare levels and coupling diagram in the case of two propagating excitations.

with some constants C_k which fulfill the normalization condition $\sum_k |C_k|^2 = 1$.

To calculate the group velocity, we assume that the spectral width of the incoming photon is smaller than the transparency window $c\Delta k_s = \Delta\omega_s < \omega_{\text{tr}}$, which is defined by $\omega_{\text{tr}} = \frac{G^2}{\gamma\sqrt{d_o}}$ [15]. Here, $d_o = L/L_{\text{abs}}$ is the optical depth and $L_{\text{abs}} = \gamma c/g^2n$ is the resonant absorption length of the medium. Since within the transparency width each k excitation is described by the corresponding dark state $|\psi_D^k\rangle$, fulfilling this condition ensures that the entire excitation will propagate as a dark state. In this case, we can treat the propagation perturbatively. Calculating the first-order energy correction resulting from the last term in (9) yields the dispersion relation $\omega(k) = \langle\psi_D^k| \sum_{k'} \hbar\omega_{k'}\hat{b}_{k'}^\dagger\hat{b}_{k'} |\psi_D^k\rangle/\hbar$. The group velocity is then given by

$$v_g^{(1)} = \frac{\partial\omega(k)}{\partial k} = \frac{\partial\langle\psi_D^k| \sum_{k'} \omega_{k'}\hat{b}_{k'}^\dagger\hat{b}_{k'} |\psi_D^k\rangle}{\partial k} = c\frac{G^2}{G^2+g^2n}, \quad (12)$$

where we used the fact that for a free field, $\omega_k = ck$.

In the next step, we consider two excitations. The corresponding coupling scheme is shown in Fig. 3. At first glance, it looks different from the corresponding coupling diagram in the single-mode case (see Fig. 2). For example, the state that contains two photonic excitations $|1_k,1_{k'},g,0\rangle$ couples now to two different states which contain an atomic excitation, namely, $|1_k,e_{k'},0\rangle$ and $|1_{k'},e_k,0\rangle$. Also the coupling constants are changed. However, if we combine these two states to a symmetric superposition state $|1,e,0\rangle_S^{kk'} = 1/\sqrt{2}(|1_k,e_{k'},0\rangle + |1_{k'},e_k,0\rangle)$ and apply this procedure to all other degenerate states, we again end up with a coupling scheme that is identical to that of the single-mode case. Most importantly, the resulting effective coupling constants between the symmetric states are the same as in the single-mode case. The corresponding dark state is then given by Eq. (6) and reads

$$|\psi_D^{kk'}\rangle = \frac{1}{\mathcal{N}}\left[\sqrt{2}G^2 |1_k 1_{k'},g,0_c\rangle + g^2n |0_s,s_k s_{k'},2_c\rangle\right.$$
$$\left. - 2Gg\sqrt{n}\frac{1}{\sqrt{2}}(|1_k,s_{k'},1_c\rangle + |1_{k'},s_k,1_c\rangle)\right]. \quad (13)$$

A general dark state containing two excitations then reads

$$|\Psi_D^{(2)}\rangle = \sum_{kk'} C_{kk'} |\psi_D^{kk'}\rangle, \tag{14}$$

in complete analogy to Eq. (11). The group velocity can be determined in a similar manner as in the single-excitation case,

$$v_g^{(2)} = \frac{\partial \langle \psi_D^{kk'} | \sum_{\tilde{k}} \omega_{\tilde{k}} \hat{b}_{\tilde{k}}^\dagger \hat{b}_{\tilde{k}} | \psi_D^{kk'} \rangle}{\partial K}$$

$$= c \frac{2G^4 + 2G^2 g^2 n}{g^4 n^2 + 4G^2 g^2 n + 2G^4}, \tag{15}$$

where the differentiation is now made with respect to the center-of-mass momentum $K = k + k'$.

The generalization to N excitations is straightforward. Start with the N-excitation dark state (7) and replace the state $|M_s, s^{N-M}, (N-M)_c\rangle$ by the symmetric state of all $\binom{N}{M}$ degenerate states. Calculate the first-order energy correction and differentiate this with respect to the center-of-mass momentum $K = k_1 + k_2 + \cdots + k_N$ to obtain the group velocity. This yields

$$\frac{v_g^{(N)}}{c} = \frac{\sum_{M=0}^{N} \frac{M}{N} (f^M s^{N-M})^2}{\sum_{M=0}^{N} (f^M s^{N-M})^2}. \tag{16}$$

The factor $\frac{M}{N}$ in the numerator results from the symmetrization procedure and can be interpreted as a weighting factor of the corresponding state to the group velocity. This means, for example, that the component of the state containing N photons contributes fully and the symmetric state with only one photon contributes with relative weight $1/N$ to the propagation velocity.

The dependence of the group velocity on the number of incoming photons according to Eq. (16) is plotted in Fig. 4. One notices that the group velocity for N photons is always smaller than the group velocity for $N + 1$ photons and that in
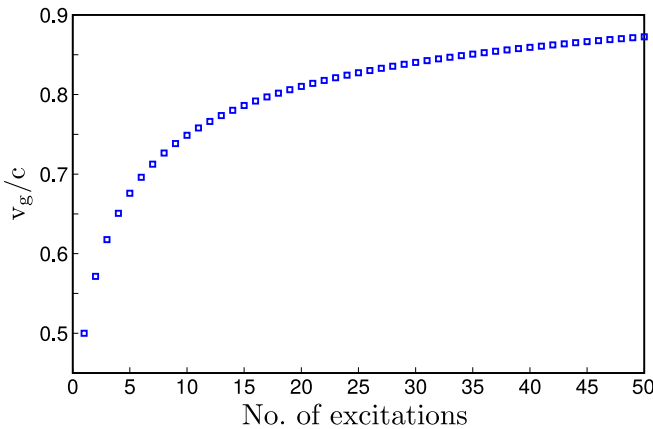

FIG. 4. The dependence of the group velocity on the number of incoming photons in the case $G = g\sqrt{n}$. The group velocity for some fixed photon number N is always larger than the one for preceding numbers and approaches the vacuum speed of light in the limit of large photon numbers N.
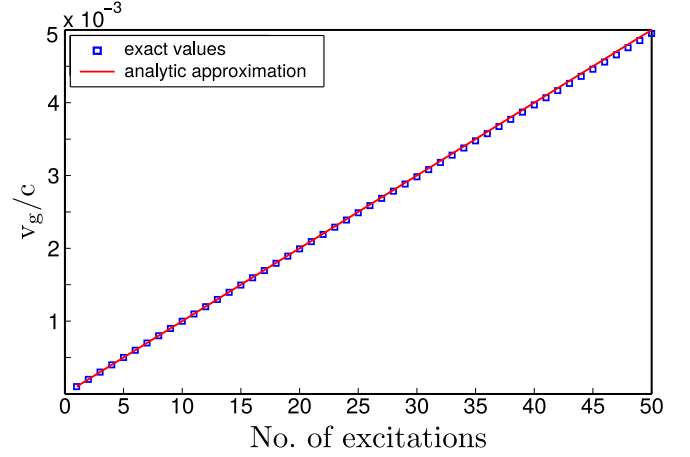

FIG. 5. The dependence of the group velocity on the number of incoming photons in the case $G = 0.01 g\sqrt{n}$ and the corresponding fit of the approximation (17).

the limit of large N the group velocity approaches the vacuum speed of light, as one would expect.

In the limit $G \ll g\sqrt{n}$, which is typically the case in experiments, we can give an analytic approximation for the group velocity,

$$\frac{v_g}{c} \approx \frac{G^2}{g^2 n} N, \tag{17}$$

i.e., the group velocity scales linearly with the number of photons. A comparison between this approximation and the full expression (16) is shown in Fig. 5.

IV. NUMERICAL RESULTS

To confirm the results derived in the previous section and to take into account boundary effects associated with the finite spatial extend of the medium, we numerically simulate the propagation of pulses with up to two photons. We perform the simulations using Hamiltonian (2) by making a wave-function ansatz and numerically integrating the corresponding Schrödinger equations for the amplitudes of the different components. The single-excitation wave function reads

$$|\psi(t)\rangle = \int d^3\mathbf{r} \frac{f(z,t)}{\sqrt{V}} \hat{\mathcal{E}}^\dagger(\mathbf{r}) |0\rangle + \int d^3\mathbf{r} \sqrt{n(\mathbf{r})} \frac{e(z,t)}{\sqrt{V}} \sigma_{eg}(\mathbf{r}) |0\rangle$$

$$+ \int d^3\mathbf{r} \sqrt{n(\mathbf{r})} \frac{s(z,t)}{\sqrt{V}} \sigma_{sg}(\mathbf{r}) a_c^\dagger |0\rangle, \tag{18}$$

where $|f(z,t)|^2$ corresponds to the probability of finding a photon at position z, and the probability of finding an atom at the same position in state $|e\rangle$ and $|s\rangle$ is given by $|e(z,t)|^2$ and $|s(z,t)|^2$, respectively. Using the commutator relations

$$[\hat{\mathcal{E}}(\mathbf{r}), \hat{\mathcal{E}}^\dagger(\mathbf{r}')] = \delta(\mathbf{r} - \mathbf{r}'), \tag{19}$$

$$[\sigma_{ij}(\mathbf{r}), \sigma_{kl}(\mathbf{r}')] = \frac{1}{n(\mathbf{r})} [\delta_{jk}\sigma_{il}(\mathbf{r}) - \delta_{il}\sigma_{kj}(\mathbf{r})]\delta(\mathbf{r} - \mathbf{r}'), \tag{20}$$

we obtain the corresponding equations of motion,

$$\partial_t f(z,t) = -c\partial_z f(z,t) + ig\sqrt{n(\mathbf{r})}e(z,t), \qquad (21)$$

$$\partial_t e(z,t) = -\gamma e(z,t) + ig\sqrt{n(\mathbf{r})}f(z,t) + iG^*s(z,t), \qquad (22)$$

$$\partial_t s(z,t) = iGe(z,t), \qquad (23)$$

where we include the decay from the excited state $|e\rangle$. These equations are equivalent to the propagation equations in the EIT case. From the EIT case, we know that if the pulses are long enough, i.e., if they fulfill the adiabaticity condition $T_p > 1/\omega_{\text{tr}}$ [15], we can adiabatically eliminate the $e(z,t)$ component. This allows us to recast the equations of motion to a single propagation equation for the $f(z,t)$ component,

namely,

$$(\partial_t + v_g\partial_z)f(z,t) = 0, \qquad (24)$$

i.e., the single-photon pulse travels through the medium without being absorbed with reduced group velocity $v_g = cG^2/(G^2 + g^2n)$, which coincides with the propagation velocity $v_g^{(1)}$ derived in the last section for the single excitation. The corresponding time delay after propagation then reads $\Delta\tau = L/v_g^{(1)}$, where L is the medium length. Using the EIT analogy, we can also describe the behavior of the pulse on the medium boundary, where the group velocity changes from c to v_g. Such a change leads to a pulse compression inside the medium by the factor v_g/c.

Let us move on to two-photon pulses. Here the wave function can be written as

$$
\begin{aligned}
|\psi(t)\rangle = {} & \frac{1}{\sqrt{2}}\int d^3\mathbf{r}\int d^3\mathbf{r}'\frac{ff(z,z',t)}{V}\hat{\mathcal{E}}^\dagger(\mathbf{r})\hat{\mathcal{E}}^\dagger(\mathbf{r}')|0\rangle + \int d^3\mathbf{r}\int d^3\mathbf{r}'\frac{ef(z,z',t)}{V}\sqrt{n(\mathbf{r})}\sigma_{eg}(\mathbf{r})\hat{\mathcal{E}}^\dagger(\mathbf{r}')|0\rangle \\
& + \frac{1}{\sqrt{2}}\int d^3\mathbf{r}\int d^3\mathbf{r}'\frac{ee(z,z',t)}{V}\sqrt{n(\mathbf{r})}\sqrt{n(\mathbf{r}')}\sigma_{eg}(\mathbf{r})\sigma_{eg}(\mathbf{r}')|0\rangle + \int d^3\mathbf{r}\int d^3\mathbf{r}'\frac{sf(z,z',t)}{V}\sqrt{n(\mathbf{r})}\sigma_{sg}(\mathbf{r})a_c^\dagger\hat{\mathcal{E}}^\dagger(\mathbf{r}')|0\rangle \\
& + \int d^3\mathbf{r}\int d^3\mathbf{r}'\frac{es(z,z',t)}{V}\sqrt{n(\mathbf{r})}\sqrt{n(\mathbf{r}')}\sigma_{eg}(\mathbf{r})\sigma_{sg}(\mathbf{r}')a_c^\dagger|0\rangle \\
& + \frac{1}{2}\int d^3\mathbf{r}\int d^3\mathbf{r}'\frac{ss(z,z',t)}{V}\sqrt{n(\mathbf{r})}\sqrt{n(\mathbf{r}')}\sigma_{sg}(\mathbf{r})\sigma_{sg}(\mathbf{r}')a_c^{\dagger 2}|0\rangle.
\end{aligned}
\qquad (25)
$$

Similar to single excitation, the absolute value squared of the coefficients gives the probability of finding the system in the corresponding state. In Fig. 6, we plot the quantity $|ff(z,z')|^2$, which is proportional to the probability of finding two photons at positions z and z'. We see that just as in the single-photon case, the two-photon pulse is compressed inside the medium. However, in addition, we recognize that the shape of the wave function is distorted after propagation through the medium. To understand how this distortion comes about, let us consider some component $ff(z_1,z_2)$. As already mentioned, the absolute value squared gives the probability of finding two photons with mutual distance $d = |z_1 - z_2|$. Initially, both photons are outside of the medium and travel with the speed of light. Then the first photon enters the medium and propagates now with the reduced group velocity $v_g^{(1)}$ until, after the time $t = d/c$, the second photon enters the medium. Since now there are two photons inside the medium, they both propagate with the group velocity $v_g^{(2)} > v_g^{(1)}$. Due to pulse compression in the medium, the distance of the two photons is reduced to $d' = dv_g^{(1)}/c$. Then, after the time $t' = (L - d')/v_g^{(2)}$, where L is the medium length, the first photon will leave the medium and the remaining photon will now propagate with the group velocity $v_g^{(1)}$ until it leaves the medium. Afterwards, both photons will again propagate with the speed of light. This shows that the amount of time that both photons propagate with the two-photon group velocity $v_g^{(2)}$ depends on their mutual distance inside the medium d'. Taking this into account, we can explain the shape distortion. The components on the first bisectrix have the smallest possible distance $d = 0$ and travel at all times with the larger group velocity $v_g^{(2)}$ and hence are more advanced in comparison to other components

with nonvanishing mutual distance. The maximal time delay between the single- and two-photon component is then

$$\Delta\tau_{12} = L\left(\frac{1}{v_g^{(1)}} - \frac{1}{v_g^{(2)}}\right) \approx \frac{1}{2}\frac{L}{c}\frac{g^2n}{G^2} = \frac{\gamma}{2G^2}d_o, \qquad (26)$$

where d_o is the optical depth of the medium. The other extreme case is when the mutual distance between two photons inside the medium becomes larger than the medium size L. Obviously these components propagate only with the velocity $v_g^{(1)}$ and therefore cannot be separated from the single-photon components. This puts a limitation on the maximal pulse length. On the other hand, one cannot use arbitrary short pulses, since those would violate the adiabaticity condition and lead to pulse absorption. Rewriting the adiabaticity condition in terms of maximal delay time, we can give an upper bound for the ratio of the maximal delay time to the pulse time,

$$\frac{\Delta\tau_{12}}{T_p} < \frac{1}{2}\sqrt{d_o}. \qquad (27)$$

In order to be able to effectively separate the single-photon component, this ratio should be larger than 1. Both conditions can only be satisfied at large optical depths.

At the end of this section, we want to make some remarks on the pulses containing more than two photons. Since the dimension of the Hilbert space grows exponentially with the number of excitations, it is clear that the wave-function ansatz becomes unattractive for more than two photons. However, we can use the mutual distance argument also in the case of multiple excitations by taking into account all possible distances between photons, e.g., the three-photon component
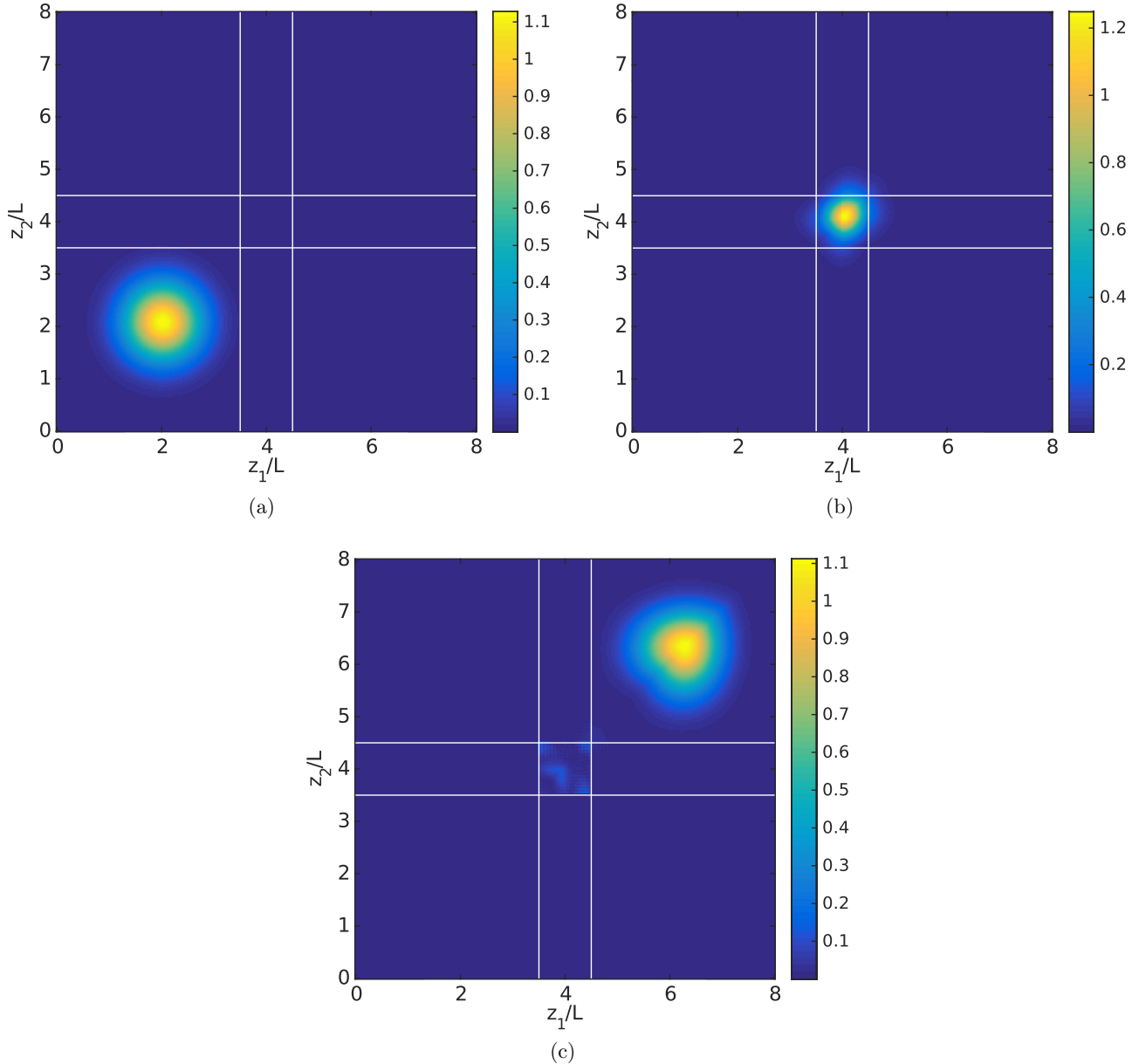
FIG. 6. The time evolution of the two-photon component $ff(z_1,z_2)$ of an initial Gaussian pulse. The parameters are $G = g\sqrt{n} = 500c/L$. The white lines denote the medium boundaries. (a) Initial Gaussian wave packet $ff(z_1,z_2) = \frac{1}{\sqrt{\pi}}e^{-2(z_1-2)^2-2(z_2-2)^2}$, (b) The two photon component after propagating inside the medium. One notices the spatial compression of the pulse, and (c) After the propagation through the medium one recognizes the distortion of the pulse shape due to non vanishing mutual distance between the two photons.

$fff(z_1,z_2,z_3)$ will propagate with the group velocity $v_g^{(3)}$, iff the largest mutual distance is smaller than the medium, i.e., all three photons are inside the medium. The group velocity will be $v_g^{(2)}$ if only two photons are present in the medium either due to the transition from free space to the medium or because the largest mutual distance is larger than the medium. For all other cases, the component will propagate with the velocity $v_g^{(1)}$. In principle, this procedure can be generalize for the N-photon component, resulting in a complicated bookkeeping for all possible distances. However, if one is mainly interested in the separation of the single-photon component from the rest, it is enough to consider single- and two-photon components, since as we see from Fig. 4 the group velocity for higher components is also higher. That means that if one manages to resolve the

single-photon component from the two-photon component, it will be automatically separated from the other components too.

V. LIMITATIONS FOR EXPERIMENTAL REALIZATION

The main limitations for the proposed scheme are the cavity damping and the decay of the excited atomic state $|e\rangle$ due to spontaneous emission. While we can safely neglect the latter one as long as we fulfill the required adiabaticity condition, the cavity decay can be an essential practical limitation. Note, however, since each k mode couples in the same way to the cavity mode, the resulting state for the induced decay from a dark state is again a dark state, e.g., the dark state containing N excitations decays to a state that contains $N-1$ excitations in

the dark state and additional atomic excitation in the $|s\rangle$ state, which due to the missing cavity photon cannot participate in the interaction any longer. That means if we have a state that is a superposition of different excitation number states, such as a coherent state, the cavity decay does not affect the spatial separation of different excitation number components; however, it leads to an exponential decay of amplitudes with a rate that is proportional to the cavity decay rate κ. To operate the filter at high *efficiency*, the cavity lifetime should be larger than the propagation time of the single photon, which is the slowest component, i.e.,

$$\kappa < \frac{v_g^{(1)}}{L} \approx \frac{G^2}{\gamma \, d_o}. \quad (28)$$

This condition can be rewritten in terms of the cavity cooperativity leading to more restrictive condition $C > d_o$ on the cavity than the usual strong-coupling condition $C > 1$. This represents a major limitation for the experimental realization. On the other hand, as argued above, the cavity decay does not affect the photon-number separation. In Sec. IV, we have seen that separation only depends on the optical depth of the medium. If we are mainly interested in the distinct *separation* of the different photon-number components, we have to fulfill the more relaxed condition $d_o \gg 1$ together with the usual strong-coupling condition $C > 1$, which is necessary for the system to build up the dark states.

Keeping that in mind, we want to discuss the possibility for an experimental realization of our proposal. State-of-the-art cavities can reach single-atom coupling strength of about $G \approx (2\pi)3$ MHz with cavity decay rates of roughly $\kappa \approx (2\pi)0.1$ MHz [16]. Using a Bose-Einstein condensate (BEC) as our three-level medium allows us to obtain the required optical depths. For example, using Rb BEC, one can reach optical depths of $d_o \approx (10-100)$ [17,18] and a single-atom cooperativity of $C \gtrsim 15$ [16,19]. A weak laser pulse can be used as the propagating probe field, i.e., we can approximate the state of the incoming field as

$$|\alpha\rangle \approx \left(1 - \frac{|\alpha|^2}{2}\right)|0\rangle + \alpha \int dz f(z) \hat{\mathcal{E}}^\dagger(z) |0\rangle$$
$$+ \frac{\alpha^2}{2} \int dz_1 \int dz_2 f(z_1) f(z_2) \hat{\mathcal{E}}^\dagger(z_1) \hat{\mathcal{E}}^\dagger(z_2) |0\rangle, \quad (29)$$

which is a good approximation for a weak coherent pulse.

This allows us to utilize the results of our calculations and extract all relevant quantities. In Fig. 7, we plot the intensity $\langle \hat{\mathcal{E}}^\dagger(t)\hat{\mathcal{E}}(t)\rangle$ of the field after propagation through the medium calculated using experimental realistic numbers from above and setting all detunings to zero. Already in this intensity plot we can recognize the spatial separation of different components. To make this separation more
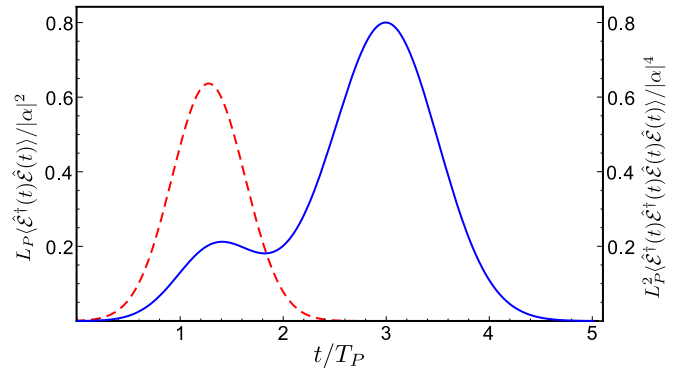

FIG. 7. Intensity (blue solid line) and two-photon component (red dashed line) of the field after propagation. The calculations are performed for a weak coherent pulse $T_p = 1$ μs containing on average $\bar{n} = |\alpha|^2 = 0.25$ photons. The other parameters are $G = (2\pi)3$ MHz and optical depth $d_o = 50$.

evident, we also plot the expectation value of the two-photon component $\langle \hat{\mathcal{E}}^\dagger(t)\hat{\mathcal{E}}^\dagger(t)\hat{\mathcal{E}}(t)\hat{\mathcal{E}}(t)\rangle$. Here we can clearly see that this component is about $\Delta\tau_{12}$ ahead of the single-photon component.

VI. CONCLUSION

In conclusion, we presented a detailed analysis of our proposal for a number-state filter for propagating light pulses based on cavity-induced transparency. Assuming adiabaticity and an infinite homogeneous medium, we derived a general expression for the dependence of the group velocity on the number of incoming photons. To take into account the effects associated with the finite medium size, we performed numerical simulations for few-photon wave packets. Using the results of these simulations, we could explain the behavior of the light pulse components with different photon numbers at the medium boundaries and derive a condition for the separation of the single-photon component from the rest. Finally, we investigated a possibility for an experimental realization of our proposal. We found that a successful implementation seems to be possible. However, in order to reach high efficiency, we have to modify the usual strong-coupling condition in terms of the cavity cooperativity $C > 1$ to the more restrictive condition $C > d_o$, where d_o is the optical depth of the medium. Note that this *efficiency* condition is, however, not a constraint for the *separation* of different photon-number components. For this, it is sufficient to fulfill less restrictive conditions: $d_o \gg 1$ and $C > 1$.

ACKNOWLEDGMENT

[1] D. Bouwmeester, A. K. Ekert, and A. Zeilinger, *The Physics of Quantum Information: Quantum Cryptography, Quantum Teleportation, Quantum Computation*, 1st ed. (Springer, New York, 2010).

[2] L. M. Duan, M. D. Lukin, J. I. Cirac, and P. Zoller, Nature (London) **414**, 413 (2001).

[3] E. Knill, R. Laflamme, and G. J. Milburn, Nature (London) **409**, 46 (2001).

[4] J. M. Raimond, M. Brune, and S. Haroche, Rev. Mod. Phys. **73**, 565 (2001).

[5] B. Peaudecerf, C. Sayrin, X. Zhou, T. Rybarczyk, S. Gleyzes, I. Dotsenko, J. M. Raimond, M. Brune, and S. Haroche, Phys. Rev. A **87**, 042320 (2013).

[6] B. T. H. Varcoe, S. Brattke, M. Weidinger, and H. Walther, Nature (London) **403**, 743 (2000).

[7] M. Hijlkema, B. Weber, H. P. Specht, S. C. Webster, A. Kuhn, and G. Rempe, Nat. Phys. **3**, 253 (2007).

[8] H. P. Specht, J. Bochmann, M. Mucke, B. Weber, E. Figueroa, D. L. Moehring, and G. Rempe, Nat. Photon. **3**, 469 (2009).

[9] M. Hofheinz, E. M. Weig, M. Ansmann, R. C. Bialczak, E. Lucero, M. Neeley, A. D. O'Connell, H. Wang, J. M. Martinis, and A. N. Cleland, Nature (London) **454**, 310 (2008).

[10] A. Holleczek, O. Barter, G. Langfahl-Klabes, and A. Kuhn, Proc. SPIE **9377**, 937709 (2015).

[11] G. Nikoghosyan and M. Fleischhauer, Phys. Rev. Lett. **105**, 013601 (2010).

[12] M. Fleischhauer, A. Imamoglu, and J. P. Marangos, Rev. Mod. Phys. **77**, 633 (2005).

[13] J. E. Field, Phys. Rev. A **47**, 5064 (1993).

[14] H. Tanji-Suzuki, W. Chen, R. Landig, J. Simon, and V. Vuletić, Science **333**, 1266 (2011).

[15] M. Fleischhauer and M. D. Lukin, Phys. Rev. A **65**, 022314 (2002).

[16] T. Donner (private communication).

[17] F. Brennecke, T. Donner, S. Ritter, T. Bourdel, M. Kohl, and T. Esslinger, Nature (London) **450**, 268 (2007).

[18] S. Zhang, J. F. Chen, C. Liu, S. Zhou, M. M. T. Loy, G. K. L. Wong, and S. Du, Rev. Sci. Instrum. **83**, 073102 (2012).

[19] Y. Colombe, T. Steinmetz, G. Dubois, F. Linke, D. Hunger, and J. Reichel, Nature (London) **450**, 272 (2007).